Astron. Astrophys. 363, 244–252 (2000)

ASTRONOMY AND ASTROPHYSICS

Photometric analysis of the eclipsing binary star AI Draconis*

Ö.L. Değirmenci[1], **Ö. Gülmen**[1], **C. Sezer**[1], **A. Erdem**[2], **and A. Devlen**[1]

[1] Ege University Observatory, Science Faculty, 35100 Izmir, Turkey
[2] Çanakkale Onsekiz Mart University, Department of Physics, Faculty of Arts and Sciences, 17100 Çanakkale, Turkey

Received 15 May 2000 / Accepted 13 September 2000

Abstract. New photometric data from the eclipsing binary star AI Draconis has been analyzed with the method of Wilson-Devinney. The system shows a period increase of about 0.91 sec per century, which corresponds to a mass transfer from the less to the more massive component at a rate of $7.5\,10^{-7}\,\mathrm{M}_\odot/\mathrm{yr}$ under the conservative mass transfer hypothesis. We also suggest that the system has an unseen component which orbits around the mass center of the triplet system with a period of about 23 yrs. We found that the projectional angular separation between the third star and eclipsing pair varies from $0\farcs048$ to $0\farcs235$. These results suggestive of a third body should be checked in the future with more sensitive observations.

Key words: stars: binaries: eclipsing – stars: individual: AI Dra

1. Introduction

The light variability of AI Draconis $(= \mathrm{HD}\,153\,345 = \mathrm{BD} + 52°2009)$ was discovered by Schilt & Hill (1938). Its Algol type eclipsing binary nature was revealed by Geyer et al. (1955).

Photoelectric light curves of the system were published by Cester (1959) (no filter), Mauder (1962) (in three intermediate filters) and Winiarski (1971) (B and V filters). Cester (1959) and Mauder (1962) analyzed their own light curves and concluded that the primary minimum was an occultation of an A0 star by a F or early G star. Furthermore, Mauder suggested that AI Dra was a semi-detached (sd) system where the secondary fills its corresponding Roche lobe. Olson & Weis (1974) classified the system as B9.6 V + F6 ÷ 7 IV using uvby and H_γ photoelectric observations. Moreover, they provided some evidence for an extended atmosphere or circumstellar material in the system. The light curves of Cester (1959) and Mauder (1962) were re-analyzed by means of Wood's model by Mezzetti et al. (1980). Their solutions pointed to a transit primary minimum and to the fact that the subgiant secondary was undersized. They obtained a converged solution with the mass ratio $q = 0.43$.

Radial velocity curves of the system were published by Wellman (see Mauder 1962), Ebbighausen (1967), Duerbeck & Teuber (1978) and Khalesseh (1999). The first three authors obtained radial velocity curves for the primary component only. However, Khalesseh succeeded in obtaining radial velocity curves for both components.

Wellman and Ebbighausen reported a mass function $f(m)$ of $0.084\,\mathrm{M}_\odot$ and $0.104\,\mathrm{M}_\odot$, respectively. Duerbeck & Teuber also obtained the mass function as $0.107 \pm 0.04\,\mathrm{M}_\odot$. Assuming the spectral types of the components as B9 V + F9 IV and taking a value of 0.46 for the mass ratio, Duerbeck & Teuber obtained the masses of the components as $M_1 = 2.3\,\mathrm{M}_\odot$ and $M_2 = 1.1\,\mathrm{M}_\odot$. However Brancewicz & Dworak (1980) classified the system as A0 V + F9 and gave $M_1 = 2.25\,\mathrm{M}_\odot$ and $M_2 = 1.55\,\mathrm{M}_\odot$. According to the catalogue of Brancewicz & Dworak, AI Dra has an Algol type light curve and is a detached binary. In the study made by Khalesseh (1999) the masses of the components are $2.99\,\mathrm{M}_\odot$ and $1.28\,\mathrm{M}_\odot$, which correspond to a mass function of $0.107\,\mathrm{M}_\odot$.

2. Observations

The photoelectric B and V observations of the system were obtained at the Ege University Observatory. The light curve observations cover 17 nights in 1993. Further, in 1991, 1992 and 1998 we observed the system over three nights to obtain the times of minimum light only. All observations were made with the 48-cm (f/13) Cassegrain telescope. The telescope was equipped with an unrefrigerated EMI 9781A photomultiplier tube for all observational nights except the night in 1998. In the 1998 observations, an SSP5-A photometer was used. To construct the light curves, a total of 440 observational points were obtained in each colour. An A0 star, BD+52°2018, was used as comparison star. BD+52°2019, an A2 star, was used as a check star. During the observations no significant light variation of the comparison and check star was found. The extinction coefficients for each colour were determined for each observational night by using the observations of the comparison star. The instrumental differential B and V magnitudes (in the sense variable minus comparison), corrected for the atmospheric extinction, are given in Table 1 (accessible in electronic form). The instrumental differential B and V light and B-V colour curves are shown in Fig. 1. The photometric phases in Table 1 and Fig. 1 are calculated with the formula (2) which is given in the next section. The depth of the

Send offprint requests to: Ö.L. Değirmenci

* Table 1 is only available electronically with the On-Line publication at http://link.springer.de/link/service/00230/

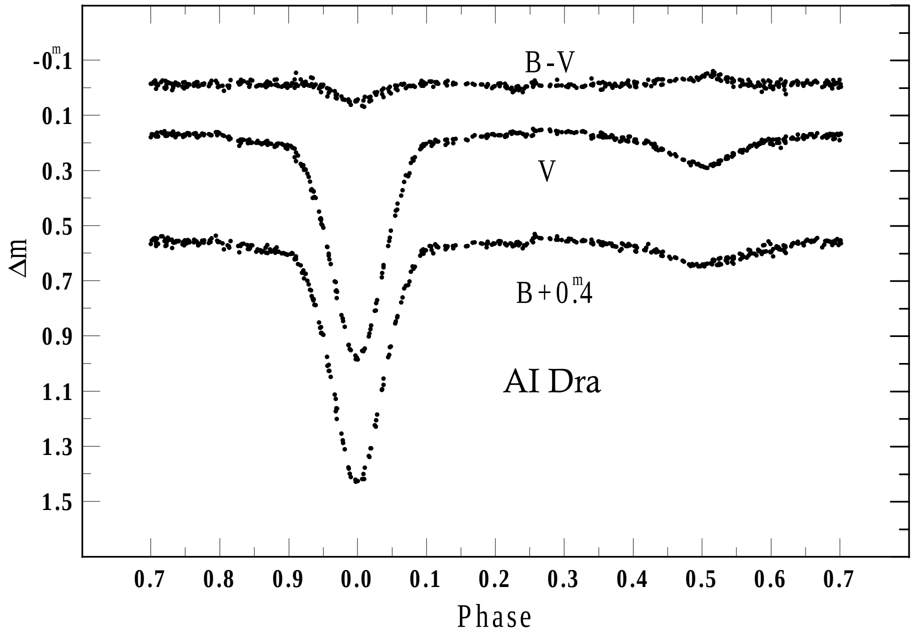

Fig. 1. Differential B and V light and B-V colour curves of AI Dra.

primary minimum is $0\overset{m}{.}877$ for B and $0\overset{m}{.}822$ for V colour while the depths of the secondary minimum are $0\overset{m}{.}091$ and $0\overset{m}{.}125$ for B and V colours, respectively. There are slight differences between the slopes of the ascending and descending branches of both minima. The ascending branches of both minima are a little steeper than the descending branches. The collapses at both shoulders of the primary minima in both colours are clearly anomalies of the light curves. These collapses may indicate circumstellar material in the system, which was pointed out by Olson & Weis (1974). This situation may indicate a gas stream flowing from the secondary, which fills the Roche lobe, to the primary component.

3. Period analysis

During the observations, we obtained four primary and two secondary times of minimum light. These times of minima and their errors, which were determined by using the method of Kwee & van Woerden (1956), are presented in Table 2. The times of minima given in Table 2 are average values of the minimum times obtained in B and V colours during the same nights. The O-C residuals given in Column 5 in Table 2 are the differences between the observed and computed times with the following ephemeris given by Winiarski (1971):

$$\text{Min I=JD (Hel)}24\ 37544.5095 + 1\overset{d}{.}1988152\, E. \tag{1}$$

We combined our times of minima with those found in the literature. Thus, we had a data set of 58 photoelectric times of minima which covering a period of about 41 yrs from 1957 to 1998. In order to calculate the photometric phases given in Table 1 and Fig. 1, we used the following formula which has been derived using the recent photoelectric times $(\text{JD} > 24\,43796)$ of minima:

$$\text{Min I=JD (Hel)}24\ 48475.3086{+}1\overset{d}{.}1988175\ \ E. \tag{2}$$
$$\pm 5 \qquad\qquad \pm 2$$

Table 2. New times of minima of AI Draconis.

JD (Hel.) 2400000+	rms	Minimum	E	O-C
48475.3077	0.0004	I	9118	$0\overset{d}{.}0012$
48837.3515	0.0003	I	9420	0.0028
49193.3997	0.0002	I	9717	0.0029
49202.394	0.001	II	9724.5	0.0061
49205.3880	0.0003	I	9727	0.0031
50969.448	0.001	II	11198.5	0.0065

The O-C diagram constructed by using the light elements given in Eq. (1) shows a sine-like variation on an upward parabola. Such a sine-like variation in which both primary and secondary minima show the same trend may be interpreted as an effect of an unseen third body in the system.

The light curve analysis (Model A) given in the following section also implies the existence of a third body in the system. Therefore, we analyzed the observed times of minima taking into account the light time effect and mass transfer from the secondary to the primary component. The times of minima of such a system are represented by the following equation:

$$T = T_o + P_o E + Q E^2 + \Delta\tau, \tag{3}$$

where T_o is the starting epoch for the primary minimum, E is the eclipse cycle number (an integer for the primary and a halved for the secondary minimum), P_o is the orbital period of the eclipsing binary at the epoch T_o,

$$2\,Q = \frac{dP}{dE} \tag{4}$$

is the rate of the real variation of the orbital period per cycle and $\Delta\tau$ is the additional time delay of any observed eclipse due to the orbit of the eclipsing pair around a third body (light-time

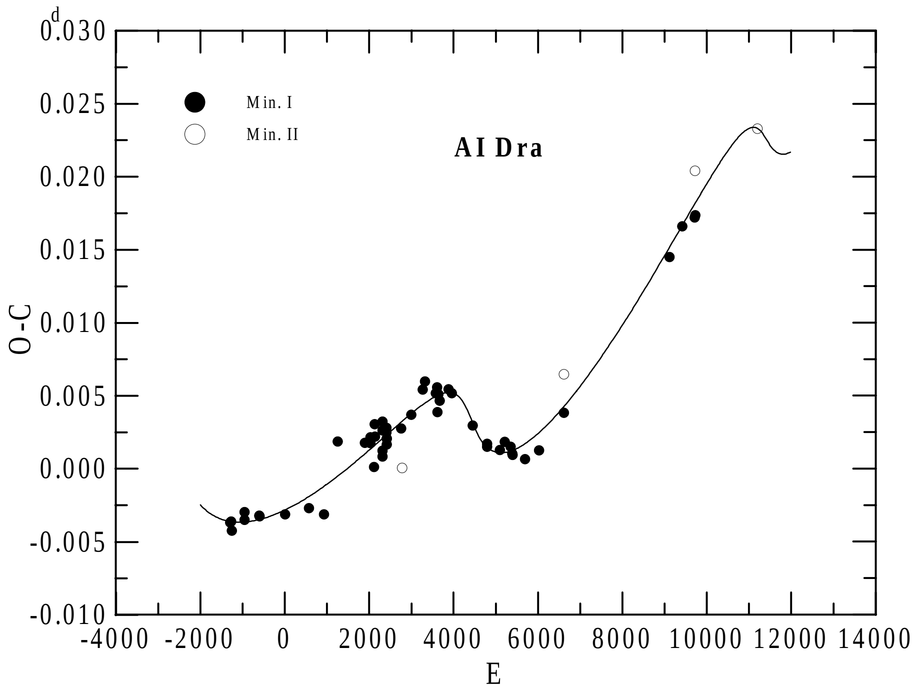

Fig. 2. The O-C diagram obtained with the photoelectric times of minima of AI Dra. The continuous curve represents the light-time effect and a real period increase.

effect). The light-time effect is given by Irwin (1959) as follows:

$$\Delta\tau = \frac{K}{\sqrt{1-e'^2\cos^2\omega'}} \times \left[\frac{1-e'^2}{1+e'\cos\nu'}\sin(\nu'+\omega')+e'\sin\omega'\right], \quad (5)$$

where

$$K = \frac{a'_{12}\sin i'\sqrt{1-e'^2\cos^2\omega'}}{2.590\times10^{10}} \quad (6)$$

is the semi-amplitude of the light-time effect in days, a_{12}, e', i' and ω' are the semi-major axis, eccentricity, inclination and the longitude of the periastron of the orbit of the eclipsing pair around the third body, respectively, and ν' is the true anomaly of the position of the eclipsing pair's mass center on the orbit. The transition time T' of the eclipsing pair's mass center from the periastron of its orbit and its orbital period P' are the secret parameters in Eq. (5).

The mass of the third body cannot be obtained from the O-C analysis without any knowledge about the inclination of its orbit. However, the O-C analysis allows us to obtain the mass function of the third body, $f(m_3)$.

In order to improve the light elements, the differential correction method was used. Applying Eq. (3) to the times of minima and using an unweighted least squares solution we obtained the parameters given in Table 3. These parameters were used to obtain the theoretical O-C curve which was plotted in Fig. 2 along with the observed values. The observed O-C values in Fig. 2 were obtained with the linear light elements of the eclipsing pair, i.e. T_o and P_o values in Table 3. The value of the quadratic coefficient Q given in Table 3 indicates a real period increase of about 0.91 s per century.

Table 3. Fitting and orbital parameters of the third body.

Parameter	Value	Standard deviation
Q (day/cycle)	1.73×10^{-10}	0.37×10^{-10}
$a_{12}\sin i'$ (km)	1.14×10^{8}	0.21×10^{8}
e'	0.66	0.14
ω' (deg)	169	10
T' (JD Hel.)	24 34411	401
P' (day)	8391	241
T_o (JD Hel.)	24 37544.5116	0.0007
P_o (day)	1.1988135	1.4×10^{-7}
$f(m_3)\,(M_\odot)$	0.0008	0.0005

4. Photometric analysis

We used the Wilson-Devinney (W-D) method (Wilson & Devinney 1971) to analyze our B and V light curves and the radial velocity curves given by Khalesseh (1999), simultaneously. We used the 1992 version of the W-D computer program (Wilson 1992) in the solutions. The method assumes the star surfaces to be equipotentials and computes the light curves as a function of the following parameters: phase shift, orbital eccentricity e and inclination i, surface potentials $\Omega_{h,c}$, flux-weighted average surface temperatures $T_{h,c}$, mass ratio $q = m_c/m_h$, unnormalized monochromatic luminosities $L_{h,c}$, linear limb darkening coefficients $x_{h,c}$, gravity darkening exponents $g_{h,c}$, bolometric albedos $A_{h,c}$ and third star's light $l3$ (if it exists). Throughout this paper, the subscripts h and c refer to the primary (hotter) and secondary (cooler) component, respectively. The W-D program gives a least-squares solution to a given light curve for the Roche model. The light curve program (LC) computes a theoretical light curve for comparison with the observations. The differential corrections program (DC) alters the light curve

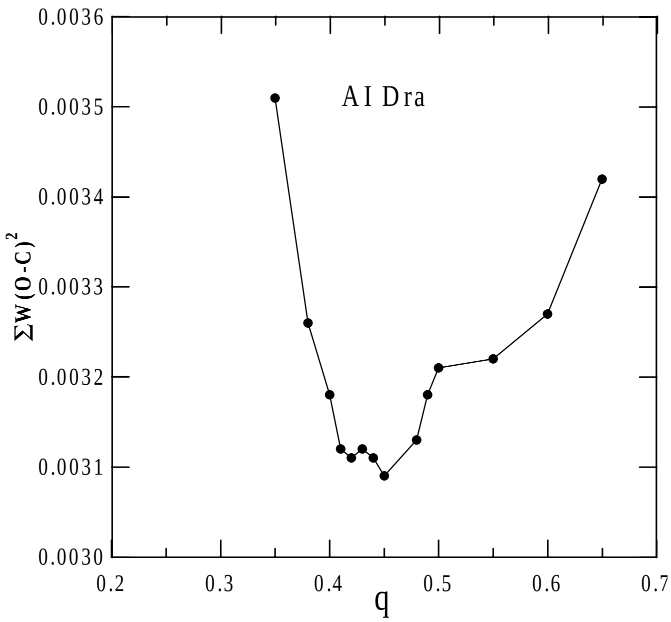

Fig. 3. The behaviour of $[\sum W(O-C)^2]$ as a function of the mass ratio.

parameters of the system in such a way that a new light curve more closely matching the observations can be generated. This process is iterated until a sufficiently good fit is obtained.

In the solutions we used normal points obtained from the individual observational points. For this, we grouped the observational points to the normal points in such a way that they accurately represent the observed light curves of the system. As a result we obtained 112 normal points for each colour and report them in Table 4. Columns 2 and 3 in Table 4 give differential B and V magnitudes while Columns 4 and 5 give the normalized B and V light intensities of the system. In order to obtain the normalized light values of the system we used mag. zero values of 0.160 mag and 0.152 mag, which correspond to the magnitudes at about 0.25 phase, for B and V colour, respectively. Each normal point in Table 4 was weighted with the number W of the individual observational points from which the normal point was constituted.

When we started to analyze the light curves, the system was known as a single line binary. To obtain the photometric mass ratio roughly, we decided to apply a q-search procedure. We carried out the q-search procedure with the V light curve by choosing phase shift, i, T_c, Ω_h, Ω_c, L_h as adjustable parameters. The solutions were started in MODE 2, which corresponds to the detached configuration, but when necessary it was switched to MODE 5, which is applied to semi-detached binaries where the secondary component fills its corresponding Roche lobe. The variation of the weighted sum of the squared residuals $[\sum W(O-C)^2]$ for the corresponding mass ratios ($q = m_c/m_h$) is shown in Fig. 3. As can be seen from the figure the lowest value of the $[\sum W(O-C)^2]$ is around q=0.43, which agrees well with the spectroscopic value given by Khalesseh (1999).

In the W-D method some parameters concerning the components should be fixed. The values of the fixed parameters may be estimated from the models by using known physical characteristics of the components. The temperature of the primary component is a very important parameter and must be chosen correctly. The temperature of the primary component was taken from Popper (1980) as equal to 9800 K, corresponding to the B9.6 V spectral class given by Olson & Weis (1974). The linear limb darkening coefficients $x_{h,c}$ were taken from Díaz-Cordovés et al. (1995). The gravity darkening exponents $g_{h,c}$ were taken from von Zeipel (1924) to be 1.0 for radiative atmospheres (primary component) and from Lucy (1967) to be 0.32 for convective atmospheres (secondary component). Also, the bolometric albedos $A_{h,c}$ were set to 1.0 and 0.5 for radiative and convective atmospheres, respectively.

In this study we solved our B and V light curves and the radial velocity curves given by Khalesseh (1999) simultaneously. The first trials for a solution were made with MODE 2 (detached configuration). Convergence to any solution in MODE 2 was very difficult and the obtained solutions were not satisfactory. Agreement between observations and theoretical light curves obtained with MODE 2, especially at the mid-eclipses, were very bad. Moreover, the method gives an inclination of about $86°$ which causes a total eclipse at the secondary minimum. This, however, does not occur in the observed light curves. Also, the MODE 2 solutions give a rather evolved configuration in which the primary and secondary components fill their corresponding Roche lobes at a rate of 0.75 and 0.87, respectively. Finally the secondary's temperature of about 5000 K obtained in MODE 2 is also not consistent with its spectral type given in the literature.

The collapses at the shoulders of the primary minima of the B and V light curves of the system are evidence of an existing gas stream flowing from the secondary, which fills its Roche lobe, to the primary component. Worek (1996) has reported some inexplicable distorted Ca II K profiles seen in the primary eclipse as well as two velocities, one at the beginning and the other at the end of the primary eclipse. According to Worek, a possible explanation for these anomalies would be circumstellar contamination. In fact Olson & Weis (1974), using narrow-band H_γ photometry, found some evidence of such material in the system. Moreover, the upward-parabolic variation in the O-C diagram given in Fig. 2 supports the mass-transfer hypothesis. Thus we completed the analysis with MODE 5.

Our period analysis is based on the existence of an unseen third body in the system. However, there is no spectroscopic evidence for it in the literature. Therefore, we decided to obtain two different models for the system: (a) with third light $l3$ (Model A), (b) without third light (Model B). The parameters a (semi-major axis of the relative orbit of the binary system), V_γ (radial velocity of the mass center of the eclipsing pair), phase shift, i, T_c, Ω_h, q, L_h and $l3$ (in Model A) were chosen as adjustable parameters. The converged solutions were obtained when the corrections of parameters became smaller than their probable errors. The results are given in Table 5. The parameters with an asterisk in Table 5 are fixed to their theoretical

Table 4. Normal points of AI Draconis

Phase	Δ B	Δ V	l_B	l_V	W
0.7063	0.1582	0.1716	0.9943	0.9894	10
0.7203	0.1553	0.1684	0.9970	0.9923	8
0.7308	0.1581	0.1681	0.9944	0.9926	8
0.7424	0.1604	0.1701	0.9923	0.9907	7
0.7527	0.1578	0.1685	0.9947	0.9922	6
0.7661	0.1606	0.1724	0.9921	0.9886	7
0.7760	0.1570	0.1690	0.9954	0.9917	4
0.7876	0.1514	0.1682	1.0006	0.9925	5
0.8004	0.1642	0.1680	0.9888	0.9927	5
0.8131	0.1703	0.1813	0.9833	0.9806	4
0.8294	0.1758	0.1956	0.9783	0.9677	5
0.8401	0.1770	0.1926	0.9772	0.9704	5
0.8496	0.1805	0.1975	0.9741	0.9661	4
0.8620	0.1908	0.2007	0.9649	0.9632	6
0.8728	0.1866	0.2040	0.9686	0.9603	5
0.8825	0.1920	0.2060	0.9638	0.9585	5
0.8894	0.2000	0.2030	0.9568	0.9612	1
0.8932	0.2010	0.2085	0.9559	0.9563	2
0.8966	0.2050	0.2153	0.9524	0.9503	3
0.9032	0.2010	0.2135	0.9559	0.9519	2
0.9074	0.2147	0.2300	0.9439	0.9376	3
0.9111	0.2237	0.2490	0.9361	0.9213	3
0.9181	0.2570	0.2800	0.9078	0.8954	2
0.9227	0.2755	0.2928	0.8925	0.8849	4
0.9276	0.3060	0.3170	0.8678	0.8654	2
0.9326	0.3468	0.3700	0.8358	0.8241	4
0.9366	0.3783	0.3868	0.8119	0.8115	4
0.9436	0.4510	0.4490	0.7593	0.7663	1
0.9471	0.4824	0.4860	0.7376	0.7406	7
0.9553	0.5760	0.5760	0.6767	0.6817	1
0.9573	0.6170	0.6025	0.6516	0.6653	4
0.9608	0.6490	0.6390	0.6327	0.6433	1
0.9680	0.7556	0.7280	0.5735	0.5927	5
0.9700	0.7640	0.7400	0.5691	0.5861	1
0.9773	0.8740	0.8360	0.5143	0.5365	3
0.9806	0.9120	0.8670	0.4966	0.5214	1
0.9877	0.9925	0.9418	0.4611	0.4867	4
0.9961	1.0220	0.9720	0.4487	0.4734	1
0.9981	1.0277	0.9833	0.4464	0.4685	3
1.0061	1.0200	0.9540	0.4496	0.4813	1
1.0087	0.9993	0.9507	0.4582	0.4827	3
1.0155	0.9360	0.9020	0.4857	0.5049	1
1.0177	0.9183	0.8763	0.4937	0.5170	3
1.0245	0.8250	0.8080	0.5380	0.5506	1
1.0265	0.8067	0.7860	0.5472	0.5618	3
1.0346	0.6950	0.6795	0.6065	0.6197	2
1.0369	0.6655	0.6475	0.6232	0.6383	2
1.0436	0.5770	0.5730	0.6761	0.6836	1
1.0462	0.5497	0.5390	0.6933	0.7053	3
1.0545	0.4515	0.4545	0.7589	0.7624	2
1.0570	0.4315	0.4310	0.7730	0.7791	2
1.0635	0.3690	0.3810	0.8188	0.8158	2
1.0681	0.3225	0.3290	0.8547	0.8559	2
1.0739	0.3085	0.3150	0.8658	0.8670	2
1.0779	0.2575	0.2640	0.9074	0.9087	2
1.0814	0.2525	0.2575	0.9116	0.9141	2
1.0898	0.2090	0.2230	0.9489	0.9436	1
1.0928	0.1925	0.2115	0.9634	0.9537	4
1.0963	0.1943	0.2070	0.9618	0.9576	3
1.1064	0.1840	0.2018	0.9710	0.9622	4
1.1141	0.1743	0.1930	0.9797	0.9701	4
1.1279	0.1783	0.1957	0.9761	0.9677	4
1.1388	0.1760	0.1907	0.9781	0.9721	3
1.1564	0.1750	0.1880	0.9790	0.9745	1
1.1589	0.1730	0.1900	0.9808	0.9727	1
1.1679	0.1605	0.1735	0.9922	0.9876	2
1.1814	0.1653	0.1747	0.9878	0.9866	3
1.1917	0.1663	0.1718	0.9869	0.9892	6
1.2037	0.1602	0.1718	0.9925	0.9892	5
1.2145	0.1680	0.1735	0.9854	0.9876	4
1.2250	0.1674	0.1626	0.9859	0.9976	5
1.2360	0.1694	0.1652	0.9841	0.9952	5
1.2522	0.1513	0.1631	1.0006	0.9971	8
1.2646	0.1455	0.1525	1.0060	1.0069	2
1.2784	0.1470	0.1545	1.0046	1.0051	2
1.2903	0.1477	0.1608	1.0040	0.9993	4
1.3040	0.1537	0.1593	0.9984	1.0006	3
1.3129	0.1547	0.1613	0.9975	0.9988	3
1.3267	0.1543	0.1590	0.9979	1.0009	4
1.3382	0.1565	0.1790	0.9959	0.9827	2
1.3453	0.1613	0.1758	0.9915	0.9856	4
1.3565	0.1663	0.1728	0.9869	0.9883	6
1.3686	0.1702	0.1792	0.9834	0.9825	5
1.3796	0.1788	0.1873	0.9756	0.9752	4
1.3902	0.1710	0.1860	0.9827	0.9763	7
1.4022	0.1812	0.1937	0.9735	0.9694	6
1.4156	0.1890	0.2000	0.9665	0.9638	2
1.4212	0.1813	0.1963	0.9734	0.9671	3
1.4315	0.1914	0.2164	0.9644	0.9494	5
1.4407	0.2025	0.2228	0.9546	0.9438	4
1.4545	0.2157	0.2397	0.9430	0.9292	3
1.4658	0.2220	0.2540	0.9376	0.9171	2
1.4781	0.2387	0.2710	0.9233	0.9028	3
1.4888	0.2423	0.2720	0.9202	0.9020	4
1.4997	0.2438	0.2856	0.9189	0.8908	5
1.5124	0.2320	0.2808	0.9290	0.8947	6
1.5226	0.2320	0.2701	0.9290	0.9036	7
1.5344	0.2218	0.2542	0.9377	0.9169	6
1.5432	0.2218	0.2433	0.9377	0.9261	6
1.5561	0.2122	0.2295	0.9461	0.9380	6
1.5667	0.2005	0.2163	0.9563	0.9495	6
1.5780	0.1968	0.2063	0.9596	0.9583	4
1.5867	0.1889	0.1958	0.9666	0.9676	8
1.5984	0.1860	0.1951	0.9692	0.9682	7
1.6091	0.1812	0.1980	0.9735	0.9656	6
1.6184	0.1832	0.1892	0.9717	0.9735	6
1.6307	0.1666	0.1836	0.9866	0.9785	5
1.6421	0.1644	0.1782	0.9886	0.9834	5
1.6538	0.1548	0.1718	0.9974	0.9892	5
1.6716	0.1580	0.1748	0.9945	0.9865	8
1.6875	0.1593	0.1738	0.9933	0.9874	8
1.6974	0.1594	0.1724	0.9932	0.9886	5

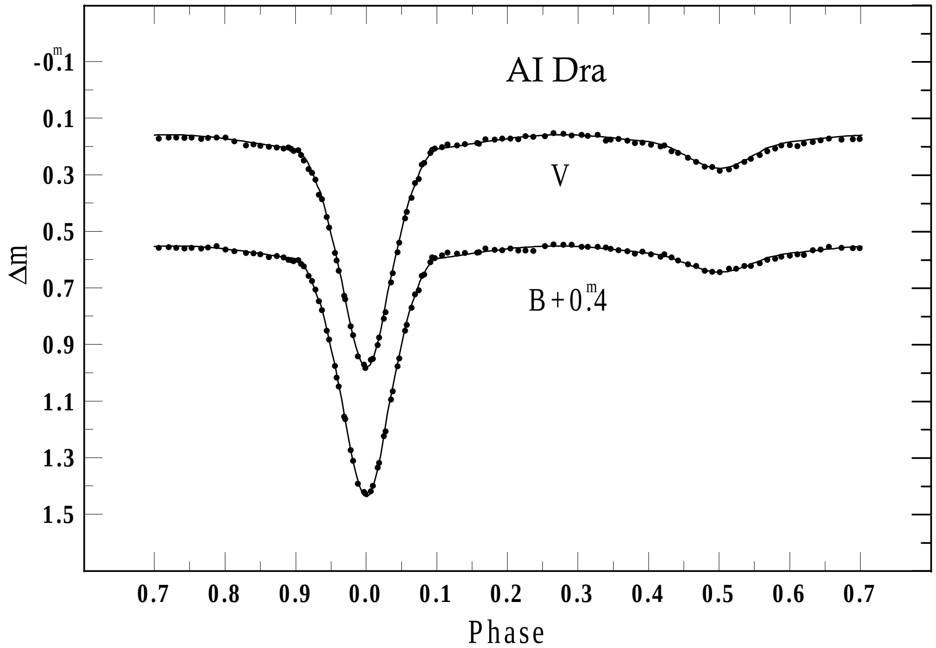

Fig. 4. Observational normal points of AI Dra and theoretical light curves obtained with the parameters of Model A.

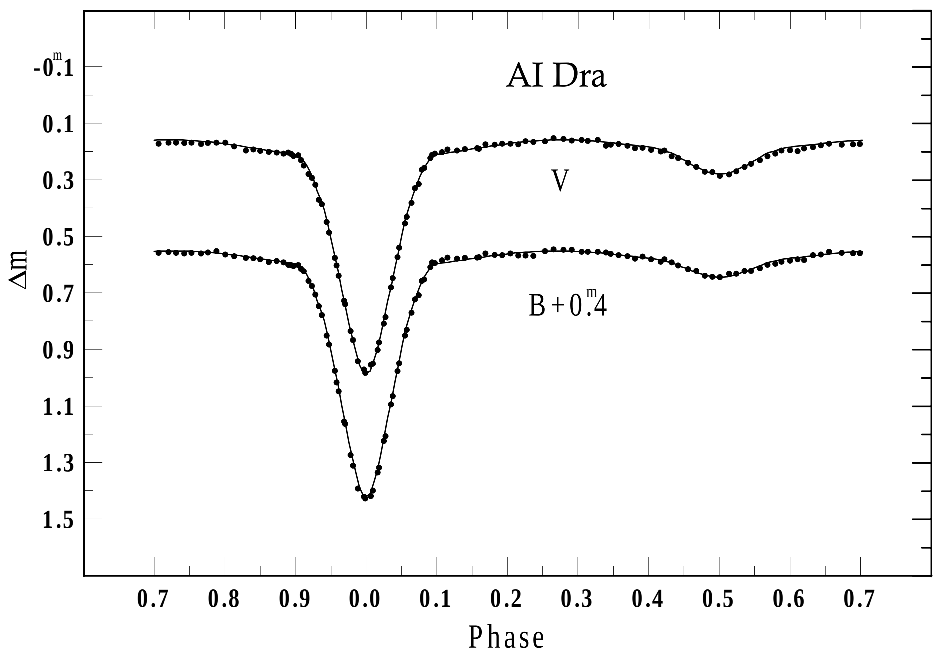

Fig. 5. Observational normal points of AI Dra and theoretical light curves obtained with the parameters of Model B.

values. The theoretical light curves calculated with the parameters of Model A and Model B are shown in Figs. 4 and 5. The comparison between observed and computed radial velocities with the parameters of the Model A are shown in Fig. 6. The agreement for both light and radial velocity curves is good. No clear evidence exists to prefer one of the models given in Table 5 over the other. Model A with the third body presented here is based only on the hypothesis that the orbital period variation of the system is due to the hypothetical third body. Of course, an alternative explanation for the period variation of the system may be suggested. To confirm the existence of the third body, spectroscopic and interferometric evidence is needed.

5. Discussion

The simultaneous solution of the light and radial velocity curves allows us to compute the absolute values of the physical parameters of the system. The absolute parameters of the system are presented in Table 6.

Our analysis gives the temperature of the secondary component as 5400 K. This value and the mass of the secondary show that the secondary component is an evolved star. The locations of the components are shown in a $logR$ vs $logM$ diagram in Fig. 7. The parabolic character in the O-C diagram indicates a mass transfer from the secondary, which fills the Roche lobe, to the primary. If we consider the simple mass transfer, Case I

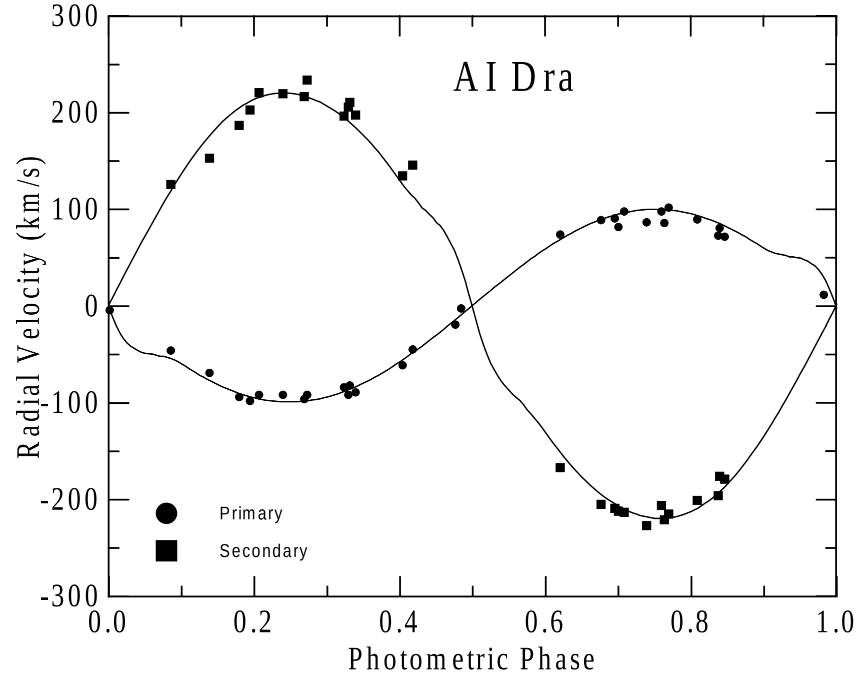

Fig. 6. Radial velocities of AI Dra given by Khalesseh (1999) and fitted curves obtained with the parameters of Model A.

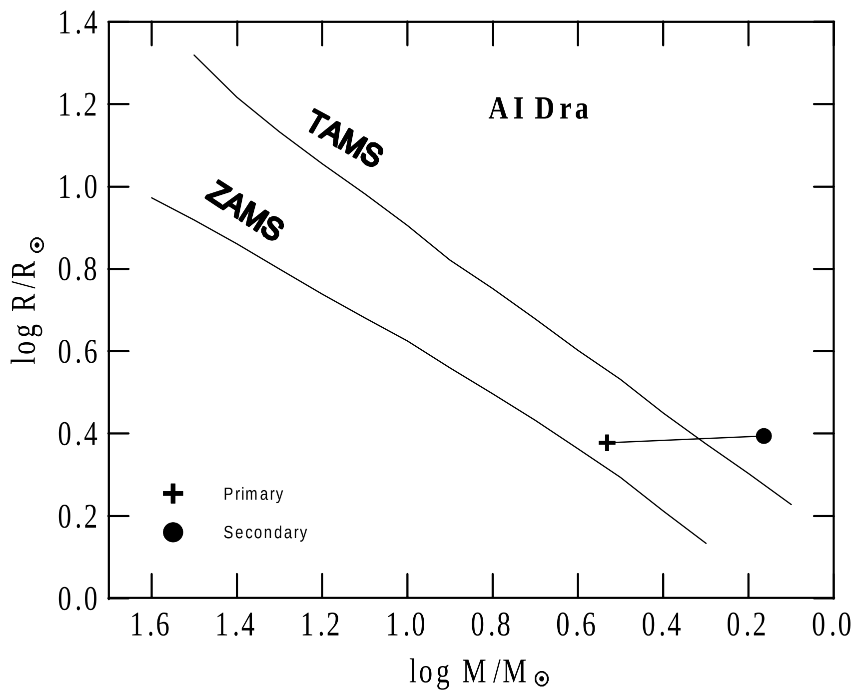

Fig. 7. The positions of the eclipsing pair's components of AI Dra in the $logR$ vs $logM$ diagram.

(see Singh & Chaubey 1986) in which the ejected material from the secondary component is falling onto the primary with no variation in the orbital angular momentum and systemic mass, we obtain a mass transfer rate of about $7.5 \times 10^{-8}\,\mathrm{M}_{\odot}/\mathrm{yr}$.

According to the table given by Straižys & Kuriliene (1981), the temperatures given in Table 5 correspond to the spectral types A0 V and G2 IV for the primary and secondary components, respectively. Also, using the light contributions of the components to the total light given in Table 5 (Model A) and assuming that the third star is a main sequence star, we obtained its spectral type as F2. Thus, according to the table given by Straižys & Kuriliene (1981), the third body has a mass of about $1.35\,\mathrm{M}_{\odot}$.

The mass function of the third body can be rewritten as follows:

$$(\sin^3 i')\, m_3^3 - f(m_3)\, m_3^2 - \; 2\, m_{12}\, f(m_3)\, m_3 - m_{12}^2\, f(m_3) \quad = 0, \qquad (7)$$

where i' is orbital inclination of the third body, m_3 and $f(m_3)$ are its mass and mass function, respectively, and $m_{12} = m_1 + m_2$ is the total mass of the eclipsing pair. When we constrain the spectral type of the third body to F2 then $i' = 10°$ from

Table 5. The results obtained by the method of Wilson-Devinney.

Parameter	Model A	Model B
a	$8.04 \pm 0.04\,R_\odot$	$8.03 \pm 0.04\,R_\odot$
V_γ	0.6 ± 0.6 km/s	0.6 ± 0.6 km/s
Phase shift	0.9991 ± 0.0001	0.9993 ± 0.0001
i	$78\overset{\circ}{.}58 \pm 0\overset{\circ}{.}02$	$78\overset{\circ}{.}03 \pm 0\overset{\circ}{.}05$
x_h^*	0.572 (B), 0.506 (V)	0.572 (B), 0.506 (V)
x_c^*	0.817 (B), 0.709 (V)	0.817 (B), 0.709 (V)
A_h^*	1.0 (B), 1.0 (V)	1.0 (B), 1.0 (V)
A_c^*	0.5 (B), 0.5 (V)	0.5 (B), 0.5 (V)
g_h^*	1.0 (B), 1.0 (V)	1.0 (B), 1.0 (V)
g_c^*	0.32 (B), 0.32 (V)	0.32 (B), 0.32 (V)
T_h^*	9800 K	9800 K
T_c	5402 ± 24 K	5404 ± 22 K
Ω_h	3.840 ± 0.012	3.842 ± 0.016
Ω_c	2.739	2.721
q	0.430 ± 0.002	0.421 ± 0.003
$L_h/(L_h + L_c + L_3)$	0.905 ± 0.004 (B)	0.938 ± 0.002 (B)
	0.852 ± 0.004 (V)	0.896 ± 0.002 (V)
$L_c/(L_h + L_c + L_3)$	0.060 (B)	0.062 (B)
	0.099 (V)	0.104 (V)
$L_3/(L_h + L_c + L_3)$	0.035 ± 0.033 (B)	–
	0.049 ± 0.033 (V)	–
$r_h(pole)$	0.2914 ± 0.0009	0.291 ± 0.0012
$r_h(point)$	0.3039 ± 0.0011	0.303 ± 0.0014
$r_h(side)$	0.2968 ± 0.0010	0.296 ± 0.0013
$r_h(back)$	0.3013 ± 0.0010	0.301 ± 0.0013
$r_c(pole)$	0.2881 ± 0.0004	0.286 ± 0.0005
$r_c(side)$	0.3004 ± 0.0005	0.299 ± 0.0005
$r_c(back)$	0.3330 ± 0.0005	0.331 ± 0.0005
$[\sum W(O-C)^2]$	0.0056	0.0054

* Fixed values during the solutions

Eq. (7). The radial velocity V_{12} of the mass center of the eclipsing pair can be represented using the well known radial velocity equation:

$$V_{12} = V_o + K' \left[e' \cos(\omega') + \cos(\nu' + \omega')\right], \quad (8)$$

where V_o is the systemic velocity of the mass center of the triplet system and K' is the semi-amplitude which is given as follows:

$$K' = \frac{2\pi}{P'} \frac{a'_{12} \sin i'}{\sqrt{1 - e'^2}}. \quad (9)$$

According to the values given in Table 3, the eclipsing pair completes its revolution around the mass center of the triplet system in about 23 yrs and its radial velocity variation has a semi-amplitude of about 1.32 km/s.

Eq. (8) gives us the possibility to check the reality of the third body. We have three radial velocity studies of the system (the Wellmann data indicated in the introduction was not found in the literature). In the first two studies, by Ebbighausen (1967) and Duerbeck & Teuber (1978), only the primary component's radial velocity curves are given. In the last study, Khalesseh (1999) obtained the radial velocity curves of both components. If two radial velocity curves are available then the simultaneous solution of these curves is more trustworthy. It is best if all radial velocity curves given in the literature can be solved with the same method for homogeneity. To this end, we resolved all radial velocity curves given in the literature by the W-D method. The resulting V_{12} values are given in Table 7 and shown in Fig. 8 as a function of time. There is no good agreement between the observed and theoretical values of the radial velocity of the eclipsing pair's mass center. The best agreement was obtained with $V_o = -0.40$ km/s. This situation must be verified by more sensitive spectroscopic observations.

Table 6. The absolute parameters of the eclipsing pair's components of AI Dra.

Parameter	Primary	Secondary
Mass $M/M_\odot$	3.40 ± 0.05	1.46 ± 0.02
Mean Radius $R/R_\odot$	2.39 ± 0.02	2.48 ± 0.02
Effective Temperature T_e (K)	9800 ± 40	5402 ± 24
Bolometric magnitude M_{bol}	$0\overset{m}{.}60 \pm 0\overset{m}{.}04$	$3\overset{m}{.}11 \pm 0\overset{m}{.}04$
Bolometric correction $B.C.$	$-0\overset{m}{.}25$	$-0\overset{m}{.}07$
Luminosity $L/L_\odot$	38.0 ± 1.7	4.4 ± 0.2
Surface gravity $\log g$ (cgs)	4.21 ± 0.04	3.81 ± 0.03

Table 7. Radial velocities V_{12} of the mass center of the eclipsing pair obtained from the solutions of the corresponding radial velocity curves with the method of Wilson-Devinney.

JD (Hel.)	V_{12} (km/s)	References to the radial velocities
24 39260	-0.5 ± 0.5	Ebbighausen (1967)
24 41800	-1.0 ± 0.5	Duerbeck & Teuber (1978)
24 46700	$+0.6 \pm 0.6$	Khalesseh (1999)

As a result, in this study, it is shown that the eclipsing binary AI Dra has a semi-detached configuration in which the secondary fills its corresponding Roche lobe and that there may be an unseen third body in the system which orbits around the common mass center of the triplet system with a period of about 23 yrs. The third body hypothesis should be checked with interferometric and spectroscopic observations. The distance of AI Dra is given as 142 ± 11 pc in the Hipparcos Catalogue. Thus, the projectional angular separation between the third star and the eclipsing pair is $0\overset{''}{.}048$ and $0\overset{''}{.}235$ at the periastron and apastron points of the orbit, respectively. These values are within the observing limits of modern technology.

Acknowledgements. This work has been supported in part by Ege University Research Foundation under contract 1997 Fen 020. The authors appreciate the valuable suggestions by Dr. P. Niarchos as a referee.

References

Brancewicz H.K., Dworak T.Z., 1980, Acta Astron. 30, 501
Cester B., 1959, Mem. Soc. Astron. Ital. 30, 287
Díaz-Cordovés J., Claret A., Giménez A., 1995, A&AS 110, 329
Duerbeck H.W., Teuber D., 1978, Acta Astron. 28, 41
Ebbighausen E.G., 1967, AJ 72, 392
Geyer E., Reim W., Remus G., Plattner D., 1955, Kl. Veröff. Remeis Sternwarte, Bamberg, 12
Irwin J.B., 1959, AJ 64, 149

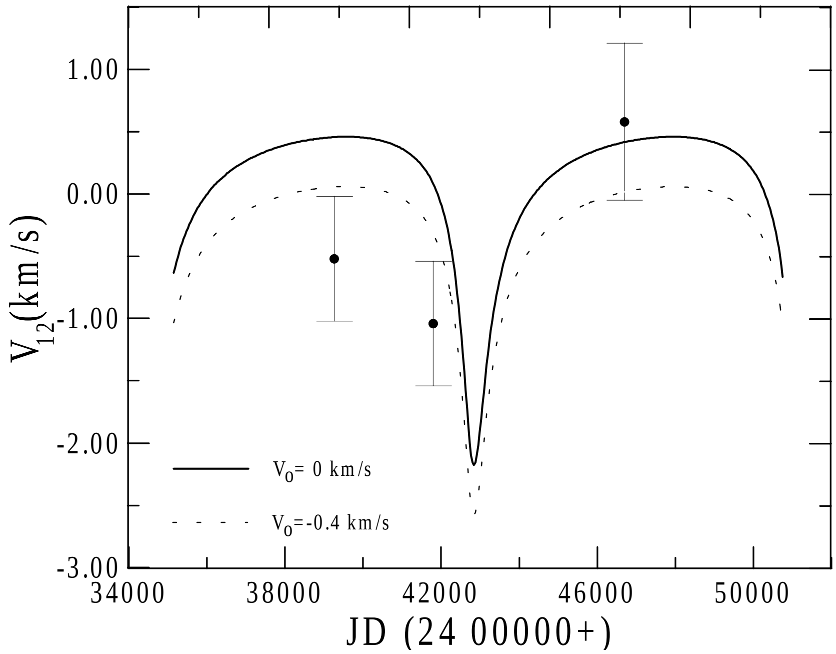

Fig. 8. Radial velocities of the eclipsing binary's mass center. Dots are the values obtained with the solutions of the different radial velocity curves of the system found from the literature and the lines represents the theoretical radial velocity curves calculated with Eq. (8) using the parameters given in Table 3.

Khalesseh B., 1999, Ap&SS 260, 299
Kwee K.K., van Woerden H., 1956, BAN 14, 131
Lucy L.B., 1967, Z. Astrophys. 65, 89
Mauder H., 1962, Z. Astrophys. 55, 59
Mezzetti M., Cester B., Giuricin G., Mardirossian, F., 1980, A&AS 39, 265
Olson E.C., Weis E.W., 1974, AJ 79, 642
Popper D.M., 1980, ARA&A 18, 115
Schilt J., Hill, S., 1938, Contrib. Rutherford Obs., 31
Singh M., Chaubey U.S., 1986, Ap&SS 124, 389
Straižys V., Kuriliene G., 1981, A&AS 80, 353
Winiarski M., 1971, Acta Astron. 21, 517
Wilson R.E., 1992, private communication
Wilson R.E., Devinney E.J., 1971, ApJ 166, 605
Worek T.F., 1996, PASP 108, 962
von Zeipel H., 1924, MNRAS 84, 665